ACS APPLIED MATERIALS & INTERFACES

Research Article

www.acsami.org

Platinum Nanoparticles: Efficient and Stable Catechol Oxidase Mimetics

Yi Liu,[†,‡] Haohao Wu,[†] Yu Chong,[†] Wayne G. Wamer,[§] Qingsu Xia,[⊥] Lining Cai,[∥] Zhihong Nie,[‡] Peter P. Fu,[*,⊥] and Jun-Jie Yin[*,†]

[†]Division of Analytical Chemistry, Office of Regulatory Science, Center for Food Safety and Applied Nutrition, U.S. Food and Drug Administration, College Park, Maryland 20740, United States

[‡]Department of Chemistry and Biochemistry, University of Maryland, College Park, Maryland 20742, United States

[§]Division of Bioanalytical Chemistry, Office of Regulatory Science, Center for Food Safety and Applied Nutrition, U.S. Food and Drug Administration, College Park, Maryland 20740, United States

[⊥]Biochemical Toxicology Division, National Center for Toxicological Research, U.S. Food and Drug Administration, Jefferson, Arkansas 72079, United States

[∥]Biotranex LLC, Monmouth Junction, New Jersey 08852, United States

Supporting Information

ABSTRACT: Although enzyme-like nanomaterials have been extensively investigated over the past decade, most research has focused on the peroxidase-like, catalase-like, or SOD-like activity of these nanomaterials. Identifying nanomaterials having oxidase-like activities has received less attention. In this study, we demonstrate that platinum nanoparticles (Pt NPs) exhibit catechol oxidase-like activity, oxidizing polyphenols into the corresponding *o*-quinones. Four unique approaches are employed to demonstrate the catechol oxidase-like activity exerted by Pt NPs. First, UV−vis spectroscopy is used to monitor the oxidation of polyphenols catalyzed by Pt NPs. Second, the oxidized products of polyphenols are identified by ultrahigh-performance liquid chromatography (UHPLC) separation followed by high-resolution mass spectrometry (HRMS) identification. Third, electron spin resonance (ESR) oximetry techniques are used to confirm the O_2 consumption during the oxidation reaction. Fourth, the intermediate products of semiquinone radicals formed during the oxidation of polyphenols are determined by ESR using spin stabilization. These results indicate Pt NPs possess catechol oxidase-like activity. Because polyphenols and related bioactive substances have been explored as potent antioxidants that could be useful for the prevention of cancer and cardiovascular diseases, and Pt NPs have been widely used in the chemical industry and medical science, it is essential to understand the potential effects of Pt NPs for altering or influencing the antioxidant activity of polyphenols.

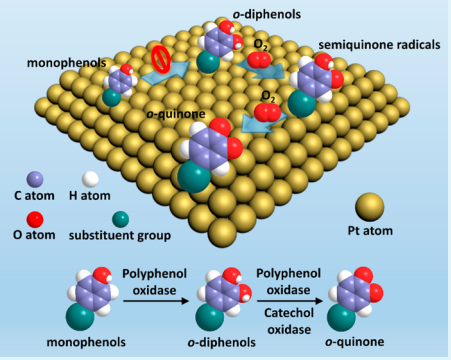

KEYWORDS: *platinum nanoparticles, heterogeneous catalysts, enzyme mimetics, catechol oxidase-like activity, oxidation of polyphenols*

1. INTRODUCTION

Nanomaterials possess many unusual physical and chemical properties, including a large surface area per unit of volume, quantum confinement, surface plasmon resonance, and superparamagnetism, which are very different from the properties exhibited by the same materials in bulk form.[1−6] Exploiting these unique properties has led to many groundbreaking findings in catalysis, photonics, optoelectronics, chemical/biological sensing, and medicine.[7−17] One area of intense scientific interest is nanomaterials that exhibit enzyme-like activity.[18−22] Although natural enzymes exhibit highly efficient catalytic activity, high substrate specificity, and high selectivity in biological reactions, most natural enzymes are proteins, which means that their catalytic activities may be destabilized by environmental conditions and subject to denaturation and digestion.[23] Purification and immobilization of natural enzymes can be labor-intensive and time-consuming, requiring complex and expensive technology such as chromatography and electrophoresis.[24−26] In contrast, nanomaterials could become stable, easy to prepare, and less costly enzyme mimetics, providing that materials can be identified which provide high catalytic efficiency, specificity, and selectivity.

To date, a wide range of nanomaterials have been identified as enzyme mimetics,[27−35] including metals,[36−38] metal oxides and sulfides,[39−42] and carbon-based nanostructures.[43−46] These nanomaterials seem to encompass an infinite number of potential structures; however, it is possible to imagine several unifying and classifying principles. Generally, the enzyme-like activities of nanomaterials can be divided into four categories: (i) peroxidase-like, (ii) oxidase-like, (iii) superoxide dismutases

Received: June 12, 2015
Accepted: August 25, 2015
Published: August 25, 2015

DOI: 10.1021/acsami.5b05180
ACS Appl. Mater. Interfaces 2015, 7, 19709−19717

(SOD)-like, and (iv) catalase-like enzyme activities.[18,47] It has been reported that carboxyl-modified graphene oxide possesses intrinsic peroxidase-like activity.[46] Other nanoparticles (NPs) that could be competitive candidates to replace SOD and catalase are CeO_2 and Co_3O_4 NPs.[20,40] Sometimes, a single nanomaterial can exhibit more than one enzyme-like property and those enzyme-like activities may change depending on external conditions. For example, nanomaterials containing precious metals, such as Au and Ag NPs, show peroxidase-like activities under acidic conditions, but catalase-like activities under alkaline conditions.[48,49] Platinum (Pt) NPs exhibit peroxidase-like activity under acidic conditions, but catalase-like activity under neutral and alkaline conditions; they show significant SOD-like activity under neutral conditions, but not under acidic conditions; they show $^1O_2$ scavenging activity both under neutral and alkaline conditions.[50] Although significant efforts have been expended to develop enzyme-like nanomaterials over the past decade, most nanomaterials research has focused on achieving peroxidase-like, catalase-like, or SOD-like activity. One very promising area has received less attention: identifying nanomaterials having oxidase-like activities.

Polyphenol oxidases are of interest due to their ubiquity and their effects on the polyphenols widely found in natural products, which have long been postulated to be beneficial to human health.[51,52] Early biochemical investigations in 1895 considered the oxidation of phenolic compounds to quinones and their subsequent polymerization to be the major path for melanin formation.[51] In humans, areas of increased accumulation of melanin in skin or the redistribution of epidermal melanin can cause dark or light patches that may be considered aesthetically displeasing.[53] In plant materials, the polymerization of polyphenols causes the enzymatic browning of fruits and vegetables, resulting in changed nutritional and organoleptic properties, diminished storage life, and product value.[54] However, other oxidations of polyphenols can be beneficial, and even considered essential to the quality of a product. In the processing of black tea, coffee, and cocoa, oxidation enhances the quality of the beverages, making products more flavorful and providing distinct organoleptic properties.[51,52] As the oxidation of polyphenols has diverse and significant biologic roles, the possibility that certain nanomaterials could exhibit oxidase-like properties must be investigated and understood, especially because it is likely that the exposure of animals, plants, and humans to nanomaterials will increase.

In this study, we report the first evidence that Pt NPs exhibit catechol oxidase enzyme-like activity. Scheme 1 illustrates the catalytic activities of Pt NPs, which can catalyze the oxidation of *o*-diphenols to *o*-quinones, but cannot catalyze the hydroxylation of monophenols to *o*-diphenols. Five of the most widespread polyphenolic dietary supplements, quercetin, L-tyrosine, L-dopa, (−)-epicatechin, and caffeic acid, were used as substrates for investigating the enzyme-like activity of Pt NPs. We investigated these oxidation processes using UV−vis spectroscopy, ultrahigh-performance liquid chromatography/high-resolution mass spectrometry (UHPLC/HRMS), and electron spin resonance (ESR) spectroscopy. Our findings provide important insights that could inform future applications of Pt NPs, which are already being used by the chemical industry in medical science and in consumer products such as dietary supplements and cosmetics.

Scheme 1. Schematic Illustration of the Catechol Oxidase-like Activities of Pt NPs

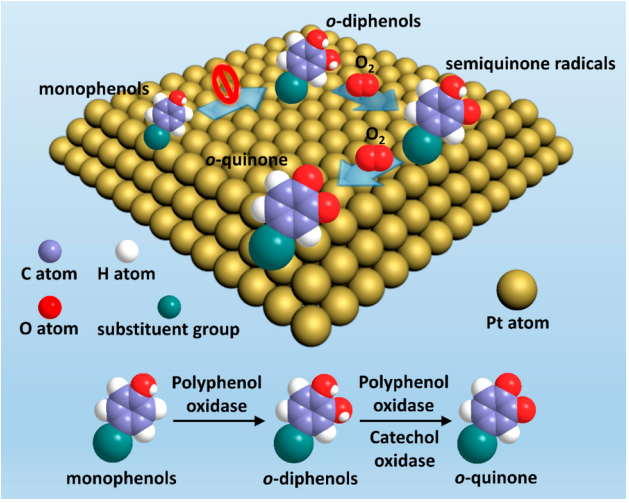

2. MATERIALS AND METHODS

2.1. Chemical and Materials. Pt NPs (5, 30, and 70 nm), coated with sodium citrate, were purchased from Nanocomposix Inc. (San Diego, CA) and used as received. 3-Carbamoyl-2,5-dihydro-2,2,5,5-tetramethyl-1H-pyrrol-1-yloxyl (CTPO), quercetin, L-tyrosine, 3,4-dihydroxy-L-phenylalanine (L-dopa), (−)-epicatechin, caffeic acid, and mushroom tyrosinase were purchased from Sigma-Aldrich (Saint Louis, MO).

2.2. Characterization. *Transmission Electron Microscopy (TEM).* TEM images were captured on a JEM 2100 FEG (JEOL) transmission electron microscope at an accelerating voltage of 200 kV located at the NanoCenter, University of Maryland, College Park, MD. To observe the morphological evolution of the Pt NPs after catalysis reaction, 1 mg/mL Pt NPs (5 nm) and 5 mM quercetin dissolved in ethanol were mixed in 1 mL of 10 mM pH 7.0 phosphate buffer solution (PBS) for 30 min and twice centrifuged (12000 rpm, 5 min). After the supernatants were decanted, 20 mL of water was added to redisperse the precipitates. The samples for TEM analysis were prepared by adding drops of the redispersed colloidal solutions onto standard carbon-coated copper grids, which were then air-dried at room temperature.

UV−vis Spectroscopy. UV−vis absorption spectra were obtained using a Varian Cary 300 spectrophotometer. To monitor the evolution of each polyphenol during the oxidation catalyzed by Pt NPs or mushroom tyrosinase, we selected the following polyphenols: quercetin, L-tyrosine, L-dopa, (−)-epicatechin, and caffeic acid, which were mixed with either Pt NPs or mushroom tyrosinase in 10 mM pH 7.0 PBS at ambient temperature. Spectra were recorded at 2 min intervals for a total of 30 min. To compare the enzymatic kinetics of Pt NPs and mushroom tyrosinase, we measured the absorption intensity of solutions containing different concentrations of quercetin and either Pt NPs or mushroom tyrosinase at 478 nm. Measurements were recorded at 0.2 min intervals for a total of 5 min. The kinetic parameters were calculated using the Michaelis−Menten equation

$$v = \frac{V_{max} \times [S]}{K_m + [S]}$$

, where v is the reaction rate, $[S]$ is the concentration of substrate, V_{max} represents the maximum rate achieved by the system at maximum (saturating) substrate concentrations. The Michaelis constant K_m is the substrate concentration at which the reaction rate is half of V_{max}.

Ultrahigh-Performance Liquid Chromatography/High-Resolution Mass Spectrometry (UHPLC/HRMS) Analysis of Quercetin Oxidation Products. Our UHPLC/HRMS system consisted of an Accela 1250 LC pump and an Accela open autosampler (Thermo Fisher Scientific, San Jose, CA, USA) coupled with a Q Exactive

DOI: 10.1021/acsami.5b05180
ACS Appl. Mater. Interfaces 2015, 7, 19709−19717

quadrupole-orbitrap mass spectrometer (Thermo Fisher Scientific, Germany). The data was acquired and processed by Xcalibur 3.0.63 and Qual Browser, respectively.

The chromatographic separations were carried out using a Waters Acquity UPLC HSS T3 reversed phase analytical column (1.8 μm, 100 mm × 2.1 mm i.d., Waters, Milford, MA, USA). The column oven temperature was set at 40 °C, and the autosampler temperature was set at 6 °C. The components were eluted by a 15 min gradient program at a flow rate of 0.40 mL/min with an injection volume of 5 μL. The mobile phase was A = 10 mM ammonium formate and 0.1% formic acid in water and B = 10 mM ammonium formate and 0.1% formic acid in methanol. The gradient parameters: 0−0.5 min, 5.0% B; 0.5−9.0 min, from 5.0% B to 95.0% B; 9.0−12.0 min, 95% B; 12.0−13.0 min, from 95% B to 5% B; and 13.0−15.0 min, 5% B.

The Q Exactive was tuned and calibrated before the measurements with Pierce ESI positive and negative ion calibration solutions (Rockford, IL, USA). The instrument was operated in negative ESI full MS−dd-MS^2 (high-resolution data-dependent product scan) acquisition mode.[55] The source parameters were sheath gas flow rate set at 60, auxiliary gas flow rate at 30, sweep gas flow rate at 2, spray voltage at −2.75 kV, capillary temperature at 350 °C; S-lens RF level at 50, and auxiliary gas heater temperature at 350 °C. For the full MS scan, the mass resolution was set at 70 000 full width at half-maximum (fwhm) at m/z 200 in the range m/z 50−750. For the dd-MS^2 scan, the mass resolution was set at 35 000, isolation window at 4.0 m/z, and NCE (normalized collision energy) at 10. Data-dependent acquisition of product scan mass spectra was initiated automatically using an inclusion list, which consists of mass (m/z), formula, species, charge, polarity, start time, end time, and optimal NCE values of precursor ions that are of interest. The inclusion list is provided in Table S1. The product scan (dd-MS^2 scan) was triggered if the given precursor ion defined in the inclusion list was detected within the 10 ppm mass error window and reached the intensity threshold (106 within 100 ms inject time).

Electron Spin Resonance (ESR). All ESR measurements were carried out using a Bruker EMX ESR spectrometer (Billerica, MA) at ambient temperature. 50 μL aliquots of control or sample solutions were put in glass capillary tubes with internal diameters of 1 mm and sealed. These capillary tubes were inserted into the ESR cavity, and the spectra were recorded at selected times. Other settings: 0.04 G field modulation, 5 G scan range, and 1 mW microwave power for ESR oximetry using spin label CTPO and 0.3 G field modulation, 20 G scan range, and 1 mW microwave power for detection of semiquinone radicals.

3. RESULTS AND DISCUSSION

3.1. Oxidation of Quercetin Catalyzed by Mushroom Tyrosinase and Pt NPs. Quercetin is a polyphenol widely distributed in many fruits, vegetables, leaves, and grains.[56] Mushroom tyrosinase, a well-known oxidase, catalyzes the hydroxylation of monophenolic compounds to *o*-diphenols and the subsequent oxidation of *o*-diphenols to *o*-quinones in the presence of O_2.[57] To discover whether or not Pt NPs can exhibit oxidase-like activity, we investigated whether the oxidation of quercetin could be catalyzed by Pt NPs. For comparison, oxidation of quercetin catalyzed by mushroom tyrosinase was also studied in parallel.

First, the oxidation process was monitored by UV−vis spectroscopy. As shown in Figure S1a, the UV−vis absorption spectrum of quercetin presented distinct absorption peaks at 256, 269, and 376 nm. These peaks can be retained for more than 1 month, indicating the good stability of quercetin exposed to air. When mushroom tyrosinase was added, the spectrum of quercetin changed. The original absorption peaks diminished, while a new absorption peak at 335 nm appeared and increased as a function of time (Figure 1a). These UV−visible absorption results are consistent with previous reports.[58]

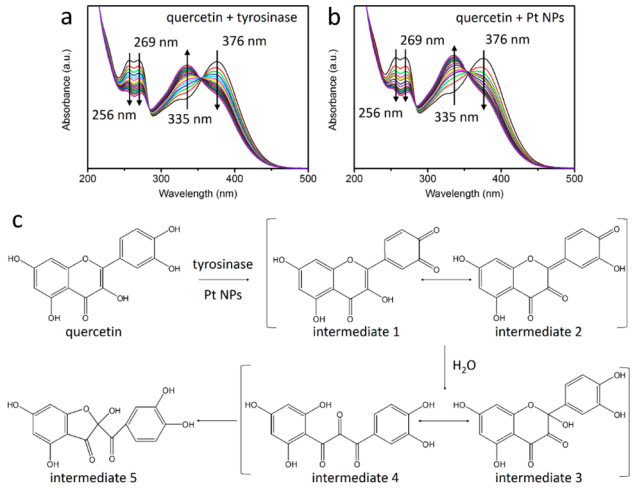

Figure 1. Evolution of UV−vis absorption spectra for quercetin in the presence of 2.7 μg/mL mushroom tyrosinase (a), and 1.4 μg/mL Pt NPs (5 nm) (b) in 10 mM phosphate buffer (pH 7.0). Quercetin was dissolved in a water/ethanol mixture (9:1; V/V) to the final concentration of 0.05 mM. The spectra were recorded at 2 min intervals for a total of 30 min. (c) Mechanism for the oxidative degradation of quercetin catalyzed by mushroom tyrosinase.

The mechanism for the oxidation of quercetin catalyzed by mushroom tyrosinase is summarized in Figure 1c: First, quercetin is oxidized into two isomeric quinones, with the structures shown as intermediate 1 and intermediate 2. These *o*-quinones are unstable, and rapidly react with water to form intermediates 3 and 4, which upon tautomerization, generate a relatively more stable oxidized product, intermediate 5. On the basis of this mechanism, the remaining solution after oxidation should be a mixture of these intermediates, whereas the spectrum of each intermediate overlaps together to form the final spectrum shown in Figure 1a.[58]

As shown in Figure 1b, the products produced by the oxidation of quercetin in the presence Pt NPs have UV−visible absorption spectra identical to the products catalyzed by mushroom tyrosinase (Figure 1a). These identical UV−visible absorption spectra suggest that Pt NPs exhibit oxidase-like activity similar to mushroom tyrosinase and the reaction products are the same mixture of intermediates shown in Figure 1c as well.

To confirm this assumption, we analyzed the oxidation products of quercetin in the presence of Pt NPs using UHPLC-HRMS. The extracted ion chromatograms and product scan mass spectra are shown in Figure 2 and Figure S2. From the results, it can be seen that (i) the UHPLC-HRMS peak eluted at 7.54 min had a deprotonated molecular ion $[M - H]^-$ at m/z 301.0354 (Figure S2b), which can be attributed to the recovered substrate quercetin; (ii) the UHPLC-HRMS peak eluted at 8.33 min had a deprotonated molecular ion $[M - H]^-$ at m/z 299.0198 (Figure S2c), which could correspond to the products intermediate 1 or intermediate 2 shown in Figure 1c; and (iii) the UHPLC-HRMS peak eluted at 5.02 min had a deprotonated molecular ion $[M - H]^-$ at m/z 317.0304 (Figure S2a), which could correlate with the product intermediate 3, intermediate 4, or intermediate 5 shown in Figure 1c. The calculated mass accuracies were all less than 1 ppm for proposed precursor ions of quercetin, intermediate 1 or 2, and intermediate 3, 4, or 5. The results of UHPLC-HRMS analysis reveal that the oxidation products of quercetin

DOI: 10.1021/acsami.5b05180
ACS Appl. Mater. Interfaces 2015, 7, 19709−19717

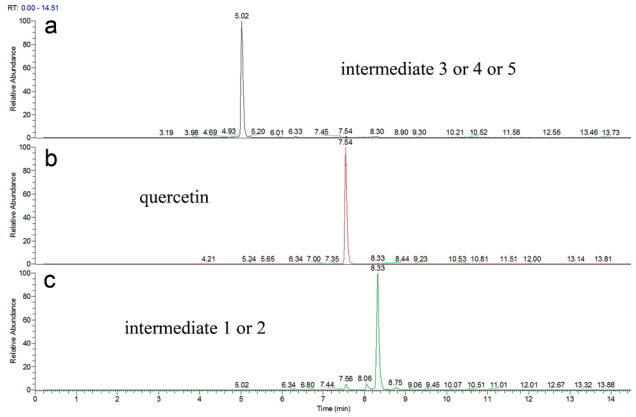

Figure 2. UHPLC-HRMS extracted ion chromatograms (mass tolerance: 5.0 ppm) of oxidation products of quercetin catalyzed by Pt NPs (5 nm): (a) $[M - H]^-$ of intermediate 3 or 4 or 5 (formula, $C_{15}H_{10}O_8$; exact mass, 317.030 29) (b) $[M - H]^-$ of quercetin (formula, $C_{15}H_{10}O_7$; exact mass, 301.035 38) (c) $[M - H]^-$ of intermediate 1 or 2 (formula, $C_{15}H_8O_7$; exact mass, 299.019 73). Structurally similar intermediates 1 and 2 have similar chromatographic and mass spectral characteristics. In addition, intermediates 3, 4, and 5 have similar chromatographic and mass spectral characteristics.

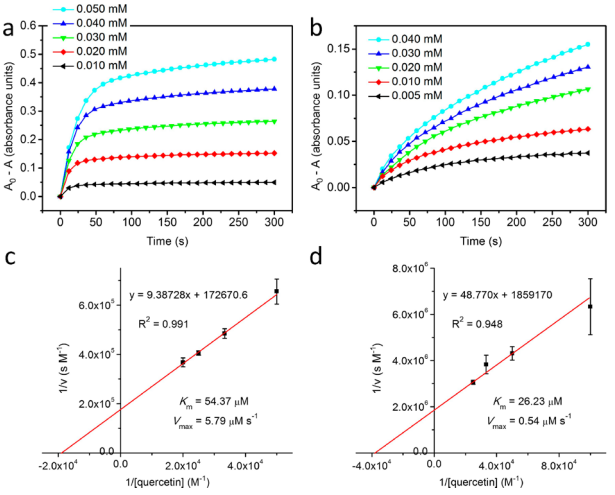

Figure 3. Evolution of absorbance for quercetin at 376 nm in the presence of 20 μg/mL Pt NPs (5 nm) (a) and 5.3 μg/mL mushroom tyrosinase (b) with different concentrations of quercetin. Double reciprocal plots for determination of kinetic constants for Pt NPs (c) and mushroom tyrosinase (d). Quercetin was dissolved in a water/ethanol mixture (9:1; V/V) with 10 mM phosphate buffer (pH 7.0).

catalyzed by Pt NPs and those catalyzed by mushroom tyrosinase are similar.

As one would expect from a catalyst, NPs with smaller diameters should exhibit higher catalytic activity under the same mass concentration, due to their higher surface area per unit of volume. We found (see Figure S3a) that 5 nm Pt NPs do show the highest catalytic activity, whereas the catalytic activity of 70 nm Pt NPs shows the weakest catalytic activity. However, surface area per unit of volume was not the only determining factor: solvents and substrates also played important roles. We will discuss this idea in more detail later.

Importantly, our TEM analyses show that Pt NPs are not consumed during these reactions: their size remains the same before and after addition, no matter what size they are (Figure S3b–e). On the basis of these results, we can conclude that Pt NPs possess oxidase-like activity similar to the activity of mushroom tyrosinase, which can catalyze the oxidation of quercetin. To the best of our knowledge, this is the first work that demonstrates the oxidase-like activity of Pt NPs.

We also investigated the effect of quercetin concentration on the catalytic reaction rate; results are shown in Figure 3. As the concentration of quercetin increases, the catalytic reaction rates of both Pt NPs and mushroom tyrosinase increase. The enzyme kinetic constant K_m (Michaelis constant) and K_{cat} (catalytic constant) are obtained to evaluate the enzyme's efficiency. K_{cat} is calculated according to $K_{cat} = V_{max}/[E]$, where $[E]$ is the Pt NPs or mushroom tyrosinase concentration and V_{max} is the maximum reaction velocity. The K_m and V_{max} for quercetin can be obtained from the double reciprocal plots of initial reaction rates over a range of quercetin concentrations (Figure 3). Catalytic parameters for the Pt NPs and mushroom tyrosinase are summarized in Table 1. For enzymes, K_m is an indicator of enzyme affinity to the substrate whereas K_{cat} represents the enzyme activity. A smaller K_m indicates a higher affinity whereas a larger K_{cat} suggests a higher enzyme activity. As shown in Table 1, the K_m of mushroom tyrosinase for quercetin is 26.23 μM (smaller than the apparent K_m (54.37 μM) of the Pt NPs), which indicates the affinity of quercetin for Pt NPs is lower

Table 1. Kinetic Parameters of Pt NPs and Mushroom Tyrosinase[a]

catalyst	C_{cat} [nM]	K_m [μM]	V_{max} [μM s^{-1}]	K_{cat} [s^{-1}]
Pt NPs	23.65	54.37	5.79	244.82
tyrosinase	44.52	26.23	0.54	12.13

[a] C_{cat} is the Pt NPs (or enzyme) concentration, K_m is the Michaelis constant, V_{max} is the maximal reaction velocity, K_{cat} is the catalytic constant.

than that of mushroom tyrosinase. However, the K_{cat} of Pt NPs and mushroom tyrosinase are 244.82 and 12.13 s^{-1} respectively, showing that Pt NPs are more efficient in catalyzing the oxidation of quercetin than mushroom tyrosinase. This K_{cat} result may not provide a direct reflection of the actual catalytic efficiency of Pt NPs and mushroom tyrosinase, as the activity of mushroom tyrosinase may be constrained by the high concentration of ethanol required in the quercetin solution, which partially deactivates the enzyme. Nonetheless, these kinetic parameters indicate that Pt NPs exhibit high stability, especially under extreme conditions.

3.2. Oxidation of L-Tyrosine and L-Dopa Catalyzed by Pt NPs and Mushroom Tyrosinase. Although we have established that Pt NPs exhibit oxidase-like activity during the oxidation of quercetin, the specificity of this catalytic activity is still unclear. Polyphenol oxidase and catechol oxidase perform different catalytic functions, so it is important to distinguish between them. Polyphenol oxidases such as mushroom tyrosinase can catalyze: (i) the *o*-hydroxylation of monophenols to *o*-diphenols as well as (ii) the oxidation of *o*-diphenols to produce *o*-quinones. In contrast, and by definition, catechol oxidase can only catalyze the oxidation of *o*-diphenols to their corresponding *o*-quinones, such as oxidation of quercetin into intermediates 1, 2, and 5 shown in Figure 1c. It cannot oxidize monophenols.

To determine whether Pt NPs are best described as polyphenol oxidase mimetics or as catechol oxidase mimetics, we compared how Pt NPs performed in oxidizing L-tyrosine and L-dopa. The molecular structures of L-tyrosine and L-dopa

DOI: 10.1021/acsami.5b05180
ACS Appl. Mater. Interfaces 2015, 7, 19709–19717

are shown in the inset of Figure 4a,b: L-tyrosine contains a phenolic hydroxyl whereas L-dopa is an *o*-diphenol. Generally,

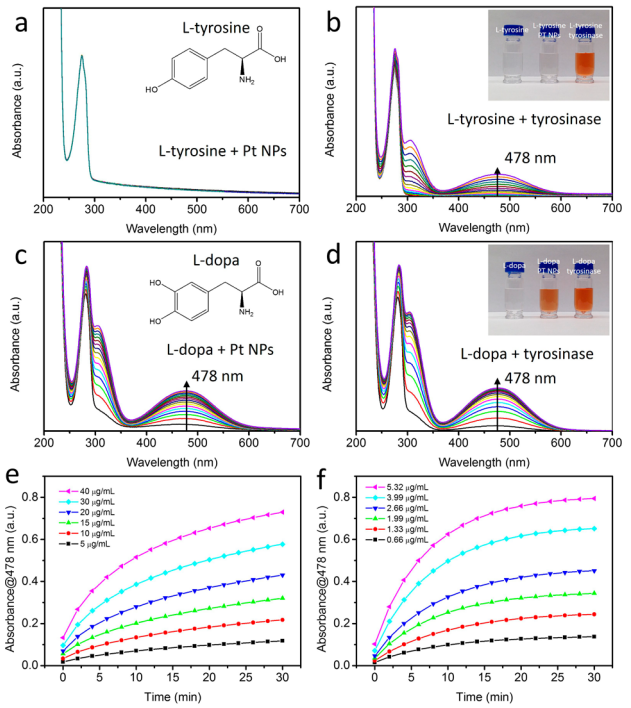

Figure 4. Evolution of UV−vis absorption spectra for L-tyrosine in the presence of 10 μg/mL Pt NPs (5 nm) (a), and 1.3 μg/mL mushroom tyrosinase (b) in 10 mM phosphate buffer (pH 7.0). Evolution of UV−vis absorption spectra for L-dopa in the presence of 10 μg/mL Pt NPs (5 nm) (c), and 1.3 μg/mL mushroom tyrosinase (d) in 10 mM phosphate buffer (pH 7.0). The final concentrations of L-tyrosine and L-dopa were 0.25 mM. The spectra were recorded at 2 min intervals for a total of 30 min. The evolution of spectra for L-dopa in the presence of different concentrations of Pt NPs (5 nm) (e) and mushroom tyrosinase (f) at 478 nm. L-Dopa was dissolved in water to the final concentration of 0.35 mM. Insets of panels a and c show the molecular structures of L-tyrosine and L-dopa. Inset of panel b shows the photographic images of solutions containing L-tyrosine, L-tyrosine and Pt NPs, L-tyrosine and mushroom tyrosinase (left to right). Inset of panel d shows the photographic images of solutions containing L-dopa, L-dopa and Pt NPs, L-dopa and mushroom tyrosinase (left to right).

polyphenol oxidases can catalyze the oxidation of L-tyrosine to L-dopa, and subsequently promote the oxidation of L-dopa to its corresponding *o*-quinone. However, as described above, catechol oxidase can only catalyze the oxidation of L-dopa to corresponding *o*-quinone; it cannot trigger the oxidation of L-tyrosine. On the basis of this mechanism, if Pt NPs can catalyze the oxidation of L-tyrosine, we can conclude that Pt NPs exhibits polyphenol oxidase-like activity. In contrast, if Pt NPs are only able to oxidize L-dopa, then, Pt NPs should be classified as mimicking catechol oxidase activity.

Figure S1b,c shows the UV−vis absorption spectra of L-tyrosine and L-dopa. Their characteristic absorption maximums are located at 275 and 281 nm, respectively. As shown in Figure 4a,c, in the presence of Pt NPs the UV−vis absorption spectra of L-tyrosine remain unchanged, whereas the oxidation of L-dopa is evidenced by the appearance of a new peak with a maximum at 478 nm. Accompanying the changes in the UV−vis absorption spectra, the original colorless solution of L-dopa becomes orange within 20 min, whereas no color variation occurs in the solution of L-tyrosine (insets of Figure 4b,d). As a control, we also tested samples containing mushroom tyrosinase in the solutions with L-tyrosine and L-dopa. As expected, the oxidation of both L-tyrosine and L-dopa can be catalyzed by mushroom tyrosinase, and the enhanced absorption at 478 nm is exhibited in the corresponding UV−vis absorption spectra (Figure 4b,d). Predictably, both of the solutions change from colorless to orange (insets of Figure 4b,d). On the basis of these UV−vis absorption spectra and photo images, we conclude that Pt NPs exhibit catechol oxidase-like activity rather than polyphenol oxidase-like activity. Furthermore, it worth noting that the oxidation products of L-dopa catalyzed by Pt NPs possess the same UV−vis absorption spectra and color as the oxidation products of L-tyrosine and L-dopa catalyzed by mushroom tyrosinase, which implies that even though their catalytic mechanisms may be different, the catalytic oxidation products of these reactions probably possess the same molecular structures. Figure 4e shows the absorbance evolution of the solution containing L-dopa and different concentrations of Pt NPs. As the concentration of Pt NPs increases, the absorption intensity at 478 nm increases, which indicates that the catechol oxidase-like activity of Pt NPs functions in a concentration-dependent manner. This relationship can also be observed when mushroom tyrosinase is used as the catalyst for the oxidation of L-dopa (Figure 4f).

Because O_2 is a reactant during oxidation, another avenue for investigating the catechol oxidase-like activity of Pt NPs is ESR oximetry in conjunction with the spin label CTPO.[59] The ESR spectra of CTPO exhibits three lines due to the hyperfine interaction of the unpaired electron with the nitrogen nucleus. Each of these lines is further split into another group of lines because of proton super hyperfine interactions. The resolution of the super hyperfine structure strongly depends on the O_2 concentration of the sample solution. Increasing O_2 concentrations result in the progressive diminution of the super hyperfine structure. In our study, the first line of hyperfine structure of the CTPO line is recorded at 3500 G. The O_2 concentration is calculated from a calibration curve relating the *K* parameter to O_2 concentration (Figure S4). As shown in Figure 5a, the ESR signal of CTPO in L-dopa solution exhibits a

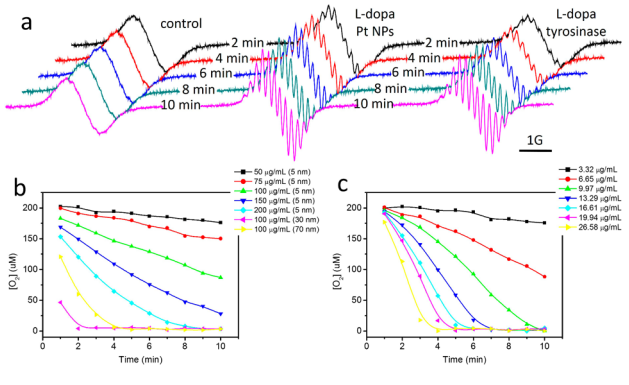

Figure 5. (a) Evolution of ESR spectra for CTPO in aqueous solution of L-dopa without catalyst, with 0.15 mg/mL Pt NPs (5 nm), and 10 μg/mL mushroom tyrosinase at different time intervals. L-Dopa was dissolved in 10 mM phosphate buffer (pH 7.0) to the final concentration of 0.5 mM. Kinetics of changes in O_2 concentration for solutions containing 0.5 mM L-dopa with different concentrations of Pt NPs (with diameters of 5, 30, and 70 nm) (b), and mushroom tyrosinase (c). L-Dopa was dissolved in 10 mM phosphate buffer (pH 7.0) to the final concentration of 0.5 mM.

DOI: 10.1021/acsami.5b05180
ACS Appl. Mater. Interfaces 2015, 7, 19709−19717

smooth profile without any super hyperfine structure, indicating that there is sufficient dissolved O_2 to cause loss of super hyperfine splitting. However, once the Pt NPs are added, those super hyperfine structures appear, accompanied by enhanced signal intensity (Figure 5a). This appearance of super hyperfine structures implies that the O_2 concentration in the solution is decreasing. Furthermore, the temporal ESR spectra evolution of the solution containing L-dopa, CTPO, and mushroom tyrosinase also exhibit a similar transition (Figure 5a). These results provide direct evidence that Pt NPs exhibit catechol oxidase-like activity, promoting the oxidation of L-dopa, which requires the consumption of O_2. As expected, the consumption of O_2 depended on the concentration of Pt NPs: as the concentration of Pt NPs increased, the rate of O_2 consumption increased as well. The size of Pt NPs also has an effect on their catechol oxidase-like activity toward L-dopa. As shown in Figure 5b, Pt NPs with diameter of 30 nm exhibited the most efficient catalytic activity, compared to bigger (70 nm) and smaller (5 nm) Pt NPs, which differs from the results observed when using quercetin as the substrate as mentioned above, surface area per unit of volume of Pt NPs is an important factor but not the only factor in determining their catalytic activities. Even though 5 nm Pt NPs possess the highest surface area per unit of volume, the solvents used with them (water for L-dopa and water/ethanol mixture for quercetin) are different, the interactions between Pt NPs and those substrates (L-dopa and quercetin) may be different as well. Each added difference will affect the final level of catalytic activities exhibited by Pt NPs.

Previous research has shown that dopa-semiquinone radicals will be formed in the early stage of L-dopa oxidation catalyzed by mushroom tyrosinase.[60] This provides a third means of demonstrating the catechol oxidase-like activity of Pt NPs on L-dopa: identifying the intermediate production of dopa-semiquinone radicals by ESR using spin stabilization. This approach uses diamagnetic metal ions, such as Zn^{2+}, to stabilize *o*-semiquinone and related radicals. The characteristic ESR spectrum of dopa-semiquinone radicals consists of eight lines with equal relative intensities, as shown in Figure S5. Using the same approach, but replacing mushroom tyrosinase with Pt NPs, we detected the identical ESR spectrum with eight lines (Figure S5). The presence of those eight lines in the ESR spectrum represents the formation of Zn^{2+}-complexed dopa-semiquinone radicals, providing additional confirmation that Pt NPs exhibit significant catechol oxidase-like activity in the oxidation of L-dopa.

Recyclability is usually regarded as an advantage of NP-based heterogeneous catalysts. Therefore, we investigated the recyclability of Pt NPs. Figure S6 shows the absorbance of the reaction solution at 478 nm as a function of reaction time in four successive cycles of catalytic reaction, using L-dopa and 30 nm Pt NPs as substrate and catalyst. After every cycle of reaction, Pt NPs were recovered from the reaction solution by centrifugation and washed with deionized water. In the first cycle, Pt NPs exhibited high catalytic activity, the absorbance of reaction at 478 nm increased rapidly with reaction time. However, the catalytic activity of Pt NPs dropped dramatically in the following reaction cycles; only 30% of original catalytic activity was retained during the fourth cycle.

This might be explained by the known effects that both centrifugation and catalytic reactions have on destabilizing the interactions between NPs and ligands. Those NPs that are not covered with ligands will aggregate, dramatically reducing their active surface areas and leading to lower catalytic activity. Several approaches can be used to overcome this problem. First, additional protective layers, such as silica, can be added to the surface of NPs to improve their stability during catalytic reactions. It is also possible to combine catalysts with magnetic NPs and then recover these NPs using external magnetic fields instead of centrifugation.

3.3. Oxidation of (−)-Epicatechin and Caffeic Acid Catalyzed by Pt NPs and Mushroom Tyrosinase.

Although the above results provide powerful demonstrations that Pt NPs exhibit catechol oxidase-like activity, if we wish to verify that Pt NPs can catalyze the oxidation of most polyphenols to their corresponding *o*-quinones, we need more examples than quercetin and L-dopa. Therefore, we selected of two the most common polyphenols consumed in daily life, (−)-epicatechin and caffeic acid (found in tea and coffee, respectively), as substrates for our next assays.

Figure S1d,e shows the UV−vis absorption spectra of (−)-epicatechin and caffeic acid. From these spectra, it can be seen that characteristic absorption maximum of (−)-epicatechin is located at 278 nm, but a new absorption peak at 433 nm appears and becomes larger as a function of time in the presence of Pt NPs (Figure 6a). We compared this to the time

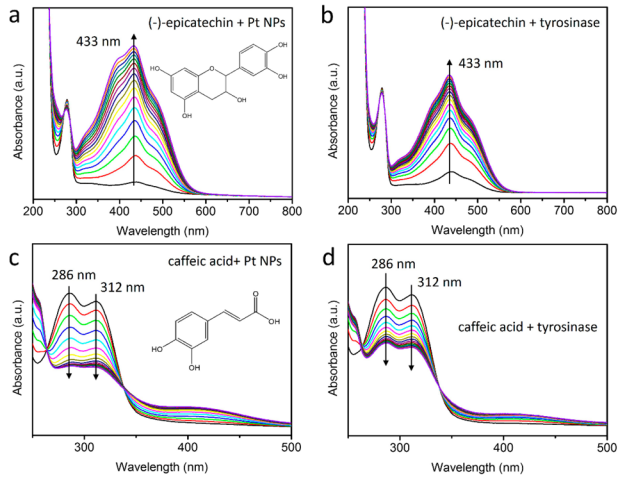

Figure 6. Evolution of UV−vis absorption spectra for (−)-epicatechin in the presence of 5 μg/mL Pt NPs (30 nm) (a), and 2.1 μg/mL mushroom tyrosinase (b) in 10 mM phosphate buffer (pH 7.0). (−)-Epicatechin was dissolved in water to the final concentration of 0.25 mM. Evolution of UV−vis absorption spectra for caffeic acid in the presence of 5 μg/mL Pt NPs (30 nm) (c), and 4 U/mL mushroom tyrosinase (d) in 10 mM phosphate buffer (pH 7.0). Caffeic acid was dissolved in water to the final concentration of 62.5 μM. The spectra were recorded at 2 min intervals for a total of 30 min. The insets of panels a and c show the molecular structures of (−)-epicatechin and caffeic acid.

dependent changes in the absorption spectra of (−)-epicatechin in the presence of mushroom tyrosinase, which exhibited a similar change (Figure 6b). The distinct absorption peaks of caffeic acid at 286, and 312 nm diminished over time after the addition of Pt NPs (Figure 6c). As expected, when mushroom tyrosinase is used as the catalyst instead of Pt NPs the same spectral change of caffeic acid can be reproduced (Figure 6d). By demonstrating the similar effects of catalysis by Pt NPs and mushroom tyrosinase on the oxidation of (−)-epicatechin and caffeic acid, we verify that the catechol oxidase-like activity of Pt NPs is not simply specific to quercetin or L-dopa, but extends to

DOI: 10.1021/acsami.5b05180
ACS Appl. Mater. Interfaces 2015, 7, 19709−19717

catalyzing the oxidation of many polyphenols to their corresponding *o*-quinones.

Scheme 1 summarizes the catalytic activities of polyphenol oxidase, catechol oxidase, and Pt NPs. Polyphenol oxidases, such as mushroom tyrosinase, are classified into the Type 3 copper protein family, which contain a binuclear copper active site coordinated by six histidines.[61,62] On the basis of the absence or presence of oxygen and the oxidation state of the copper ions [Cu(II)/Cu(I)], there are four different forms called deoxy-, oxy-, met-, and deact-tyrosinase. These forms are interconvertible, such that each form can not only initiate the hydroxylation of monophenols to *o*-diphenols but also catalyze the subsequent oxidation of *o*-diphenols to *o*-quinones.[63,64] Although catechol oxidase has the same active site, due to differences in its crystal structure it can only catalyze the oxidation of *o*-diphenols to the corresponding *o*-quinones.[65,66] However, the catalytic mechanism by which Pt NPs act on *o*-diphenols is totally different. Platinum is known to activate alcohols and molecular oxygen under close to ambient conditions and produce the corresponding carbonyl compounds in high yields, followed by a classic dehydrogenation mechanism.[67] It is possible that the oxidation of *o*-diphenols catalyzed by Pt NPs follow the same pathway. Recent studies on phenols have shown that phenols substituted with electron-releasing groups, such as hydroxyls, possess lower reduction potentials compared with unsubstituted phenols.[68] This may explain why Pt NPs can catalyze the oxidation of *o*-diphenols but not monophenols.

CONCLUSION

We have demonstrated for the first time that Pt NPs exhibit catechol oxidase-like activity, catalyzing the oxidation of polyphenols to corresponding *o*-quinones in the presence of O_2. Using UV−vis spectroscopy, UHPLC-HRMS analysis, and ESR to monitor the oxidation of polyphenols, we confirmed that Pt NPs are capable of oxidizing *o*-diphenols to *o*-quinones. However, they are unable to catalyze the hydroxylation of monophenols to *o*-diphenols, which confirms that the enzyme-like activity exhibited by Pt NPs is more similar to that of catechol than to polyphenol oxidase. Furthermore, we establish that Pt NPs are more efficient in catalyzing the oxidation of polyphenols (e.g., quercetin) than the natural enzyme mushroom tyrosinase.

Manufacturers of dietary supplements and cosmetics are increasingly interested in using Pt NPs and other nanomaterials in their products. Therefore, it is extremely important to understand the chemical and biological effects of Pt NPs and how these effects may be altered by environmental conditions. Platinum nanoparticles have been shown to mimic the catalytic activities of peroxidases, oxidases, SOD, and catalases.[50] Our results demonstrate that Pt NPs also exhibit catechol oxidase activity. Because oxidation of catechols underlies many important biological functions, the catechol oxidase activity of Pt NPs may alter the performance of products.

A number of existing dietary supplements and cosmetics contain antioxidants having the catechol moiety. Through their catechol oxidase activity, Pt NPs may diminish their antioxidant properties and could thereby alter the performance of the product or its long-term effects. In addition, because oxidation of L-dopa is a critical step in the formation of melanin, Pt NPs in skin care products may have effects on cutaneous melanization (tanning). Our results will be valuable in investigating these potentially significant effects of Pt NPs in consumer products and guiding future applications of Pt NPs.

ASSOCIATED CONTENT

Supporting Information

The Supporting Information is available free of charge on the ACS Publications website at DOI: 10.1021/acsami.5b05180.

UV−vis spectra of quercetin, L-dopa, tyrosine, (−)-epicatechin, and caffeic acid. Mass spectra of quercetin oxidation products. TEM images of Pt NPs before and after catalytic reaction. ESR spectra of Zn^{2+}-complexed dopa-semiquinone. Evolution of absorbance for L-dopa in the presence of Pt NPs in four successive cycle catalytic reaction (PDF).

AUTHOR INFORMATION

Corresponding Authors

*J.-J. Yin. Tel. +240-401-1991. E-mail: junjie.yin@fda.hhs.gov. Fax: +201-436-2624.

*P. P. Fu. Tel. +870-54-7207. E-mail: peter.fu@fda.hhs.gov. Fax: +870-543-7136.

Notes

The authors declare no competing financial interest.

ACKNOWLEDGMENTS

This work is supported by the NSF career award (DMR-1255377), startup funds from the University of Maryland, and the Joint Institute for Food Safety and Nutrition, University of Maryland, College Park, MD through a cooperative agreement funded by the FDA, Grant no. 5U01FD001418 (LY). Support was also received through a regulatory science grant under the FDA Nanotechnology CORES Program. We gratefully acknowledge Wanlong Zhou and Perry Wang (Office of Regulatory Science, Center for Food Safety and Applied Nutrition/FDA) for their expert assistance in performing UHPLC-HRMS analyses. We are also grateful to Lili Fox Vélez for her editorial support. This paper is not an official U.S. FDA guidance or policy statement. No official support or endorsement by the U.S. FDA is intended or should be inferred.

REFERENCES

(1) Burda, C.; Chen, X. B.; Narayanan, R.; El-Sayed, M. A. Chemistry and Properties of Nanocrystals of Different Shapes. *Chem. Rev.* **2005**, *105*, 1025−1102.

(2) Alivisatos, A. P. Semiconductor Clusters, Nanocrystals, and Quantum Dots. *Science* **1996**, *271*, 933−937.

(3) Heath, J. R. The Chemistry of Size and Order on a Nanometer Scale. *Science* **1995**, *270*, 1315−1316.

(4) Eustis, S.; El-Sayed, M. A. Why Gold Nanoparticles are More Precious than Pretty Gold: Noble Metal Surface Plasmon Resonance and Its Enhancement of the Radiative and Nonradiative Properties of Nanocrystals of Different Shapes. *Chem. Soc. Rev.* **2006**, *35*, 209−217.

(5) Hutter, E.; Fendler, J. H. Exploitation of Localized Surface Plasmon Resonance. *Adv. Mater.* **2004**, *16*, 1685−1706.

(6) Jeong, U.; Teng, X. W.; Wang, Y.; Yang, H.; Xia, Y. N. Superparamagnetic Colloids: Controlled Synthesis and Niche Applications. *Adv. Mater.* **2007**, *19*, 33−60.

(7) Lim, B.; Jiang, M. J.; Camargo, P. H. C.; Cho, E. C.; Tao, J.; Lu, X. M.; Zhu, Y. M.; Xia, Y. N. Pd-Pt Bimetallic Nanodendrites with High Activity for Oxygen Reduction. *Science* **2009**, *324*, 1302−1305.

(8) Astruc, D.; Lu, F.; Aranzaes, J. R. Nanoparticles as Recyclable Catalysts: The Frontier between Homogeneous and Heterogeneous Catalysis. *Angew. Chem., Int. Ed.* **2005**, *44*, 7852−7872.

DOI: 10.1021/acsami.5b05180
ACS Appl. Mater. Interfaces 2015, 7, 19709−19717

(9) Barnes, W. L.; Dereux, A.; Ebbesen, T. W. Surface Plasmon Subwavelength Optics. *Nature* **2003**, *424*, 824−830.
(10) Gudiksen, M. S.; Lauhon, L. J.; Wang, J.; Smith, D. C.; Lieber, C. M. Growth of Nanowire Superlattice Structures for Nanoscale Photonics and Electronics. *Nature* **2002**, *415*, 617−620.
(11) Wang, Q. H.; Kalantar-Zadeh, K.; Kis, A.; Coleman, J. N.; Strano, M. S. Electronics and Optoelectronics of Two-Dimensional Transition Metal Dichalcogenides. *Nat. Nanotechnol.* **2012**, *7*, 699−712.
(12) Bonaccorso, F.; Sun, Z.; Hasan, T.; Ferrari, A. C. Graphene Photonics and Optoelectronics. *Nat. Photonics* **2010**, *4*, 611−622.
(13) Anker, J. N.; Hall, W. P.; Lyandres, O.; Shah, N. C.; Zhao, J.; Van Duyne, R. P. Biosensing with Plasmonic Nanosensors. *Nat. Mater.* **2008**, *7*, 442−453.
(14) Homola, J. Surface Plasmon Resonance Sensors for Detection of Chemical and Biological Species. *Chem. Rev.* **2008**, *108*, 462−493.
(15) Rosi, N. L.; Mirkin, C. A. Nanostructures in Biodiagnostics. *Chem. Rev.* **2005**, *105*, 1547−1562.
(16) Boisselier, E.; Astruc, D. Gold Nanoparticles in Nanomedicine: Preparations, Imaging, Diagnostics, Therapies and Toxicity. *Chem. Soc. Rev.* **2009**, *38*, 1759−1782.
(17) Fan, Z.; Fu, P. P.; Yu, H.; Ray, P. C. Theranostic Nanomedicine for Cancer Detection and Treatment. *J. Food Drug Anal.* **2014**, *22*, 3−17.
(18) Wei, H.; Wang, E. K. Nanomaterials with Enzyme-Like Characteristics (Nanozymes): Next-Generation Artificial Enzymes. *Chem. Soc. Rev.* **2013**, *42*, 6060−6093.
(19) Shi, W. B.; Zhang, X. D.; He, S. H.; Huang, Y. M. $CoFe_2O_4$ Magnetic Nanoparticles as a Peroxidase Mimic Mediated Chemiluminescence for Hydrogen Peroxide and Glucose. *Chem. Commun.* **2011**, *47*, 10785−10787.
(20) Korsvik, C.; Patil, S.; Seal, S.; Self, W. T. Superoxide Dismutase Mimetic Properties Exhibited by Vacancy Engineered Ceria Nanoparticles. *Chem. Commun.* **2007**, *43*, 1056−1058.
(21) Jv, Y.; Li, B. X.; Cao, R. Positively-Charged Gold Nanoparticles as Peroxidiase Mimic and Their Application in Hydrogen Peroxide and Glucose Detection. *Chem. Commun.* **2010**, *46*, 8017−8019.
(22) Dai, Z. H.; Liu, S. H.; Bao, J. C.; Ju, H. X. Nanostructured FeS as a Mimic Peroxidase for Biocatalysis and Biosensing. *Chem. - Eur. J.* **2009**, *15*, 4321−4326.
(23) Iyer, P. V.; Ananthanarayan, L. Enzyme Stability and Stabilization - Aqueous and Non-Aqueous Environment. *Process Biochem.* **2008**, *43*, 1019−1032.
(24) Mateo, C.; Palomo, J. M.; Fernandez-Lorente, G.; Guisan, J. M.; Fernandez-Lafuente, R. Improvement of Enzyme Activity, Stability and Selectivity via Immobilization Techniques. *Enzyme Microb. Technol.* **2007**, *40*, 1451−1463.
(25) Charcosset, C. Purification of Proteins by Membrane Chromatography. *J. Chem. Technol. Biotechnol.* **1998**, *71*, 95−110.
(26) Schagger, H.; Cramer, W. A.; Vonjagow, G. Analysis of Molecular Masses and Oligomeric States of Protein Complexes by Blue Native Electrophoresis and Isolation of Membrane-Protein Complexes by 2-Dimensional Native Electrophoresis. *Anal. Biochem.* **1994**, *217*, 220−230.
(27) Chen, J.; Patil, S.; Seal, S.; McGinnis, J. F. Rare Earth Nanoparticles Prevent Retinal Degeneration Induced by Intracellular Peroxides. *Nat. Nanotechnol.* **2006**, *1*, 142−150.
(28) Silva, G. A. Nanomedicine: Seeing the Benefits of Ceria. *Nat. Nanotechnol.* **2006**, *1*, 92−94.
(29) Xia, T.; Kovochich, M.; Liong, M.; Mädler, L.; Gilbert, B.; Shi, H.; Yeh, J. I.; Zink, J. I.; Nel, A. E. Comparison of the Mechanism of Toxicity of Zinc Oxide and Cerium Oxide Nanoparticles Based on Dissolution and Oxidative Stress Properties. *ACS Nano* **2008**, *2*, 2121−2134.
(30) Celardo, I.; De Nicola, M.; Mandoli, C.; Pedersen, J. Z.; Traversa, E.; Ghibelli, L. Ce^{3+} Ions Determine Redox-Dependent Anti-apoptotic Effect of Cerium Oxide Nanoparticles. *ACS Nano* **2011**, *5*, 4537−4549.
(31) Gao, L.; Zhuang, J.; Nie, L.; Zhang, J.; Zhang, Y.; Gu, N.; Wang, T.; Feng, J.; Yang, D.; Perrett, S.; Yan, X. Intrinsic Peroxidase-Like Activity of Ferromagnetic Nanoparticles. *Nat. Nanotechnol.* **2007**, *2*, 577−583.
(32) Perez, J. M. Iron Oxide Nanoparticles: Hidden Talent. *Nat. Nanotechnol.* **2007**, *2*, 535−536.
(33) Fan, K.; Cao, C.; Pan, Y.; Lu, D.; Yang, D.; Feng, J.; Song, L.; Liang, M.; Yan, X. Magnetoferritin Nanoparticles for Targeting and Visualizing Tumour Tissues. *Nat. Nanotechnol.* **2012**, *7*, 765−765.
(34) Chen, Z.; Yin, J.-J.; Zhou, Y.-T.; Zhang, Y.; Song, L.; Song, M.; Hu, S.; Gu, N. Dual Enzyme-Like Activities of Iron Oxide Nanoparticles and Their Implication for Diminishing Cytotoxicity. *ACS Nano* **2012**, *6*, 4001−4012.
(35) Liu, M.; Zhao, H.; Chen, S.; Yu, H.; Quan, X. Interface Engineering Catalytic Graphene for Smart Colorimetric Biosensing. *ACS Nano* **2012**, *6*, 3142−3151.
(36) Long, Y. J.; Li, Y. F.; Liu, Y.; Zheng, J. J.; Tang, J.; Huang, C. Z. Visual Observation of the Mercury-Stimulated Peroxidase Mimetic Activity of Gold Nanoparticles. *Chem. Commun.* **2011**, *47*, 11939−11941.
(37) Wang, S.; Chen, W.; Liu, A.-L.; Hong, L.; Deng, H.-H.; Lin, X.-H. Comparison of the Peroxidase-Like Activity of Unmodified, Amino-Modified, and Citrate-Capped Gold Nanoparticles. *ChemPhysChem* **2012**, *13*, 1199−1204.
(38) Fan, J.; Yin, J.-J.; Ning, B.; Wu, X.; Hu, Y.; Ferrari, M.; Anderson, G. J.; Wei, J.; Zhao, Y.; Nie, G. Direct Evidence for Catalase and Peroxidase Activities of Ferritin-Platinum Nanoparticles. *Biomaterials* **2011**, *32*, 1611−1618.
(39) Natalio, F.; Andre, R.; Hartog, A. F.; Stoll, B.; Jochum, K. P.; Wever, R.; Tremel, W. Vanadium Pentoxide Nanoparticles Mimic Vanadium Haloperoxidases and Thwart Biofilm Formation. *Nat. Nanotechnol.* **2012**, *7*, 530−535.
(40) Mu, J.; Wang, Y.; Zhao, M.; Zhang, L. Intrinsic Peroxidase-Like Activity and Catalase-Like Activity of Co_3O_4 Nanoparticles. *Chem. Commun.* **2012**, *48*, 2540−2542.
(41) André, R.; Natálio, F.; Humanes, M.; Leppin, J.; Heinze, K.; Wever, R.; Schröder, H. C.; Müller, W. E. G.; Tremel, W. V_2O_5 Nanowires with an Intrinsic Peroxidase-Like Activity. *Adv. Funct. Mater.* **2011**, *21*, 501−509.
(42) Asati, A.; Santra, S.; Kaittanis, C.; Nath, S.; Perez, J. M. Oxidase-Like Activity of Polymer-Coated Cerium Oxide Nanoparticles. *Angew. Chem., Int. Ed.* **2009**, *48*, 2308−2312.
(43) Liu, S.; Tian, J.; Wang, L.; Luo, Y.; Sun, X. A General Strategy for the Production of Photoluminescent Carbon Nitride Dots from Organic Amines and Their Application as Novel Peroxidase-Like Catalysts for Colorimetric Detection of H_2O_2 and Glucose. *RSC Adv.* **2012**, *2*, 411−413.
(44) Shi, W.; Wang, Q.; Long, Y.; Cheng, Z.; Chen, S.; Zheng, H.; Huang, Y. Carbon Nanodots as Peroxidase Mimetics and Their Applications to Glucose Detection. *Chem. Commun.* **2011**, *47*, 6695−6697.
(45) Wang, X.; Qu, K.; Xu, B.; Ren, J.; Qu, X. Multicolor Luminescent Carbon Nanoparticles: Synthesis, Supramolecular Assembly with Porphyrin, Intrinsic Peroxidase-Like Catalytic Activity and Applications. *Nano Res.* **2011**, *4*, 908−920.
(46) Song, Y.; Qu, K.; Zhao, C.; Ren, J.; Qu, X. Graphene Oxide: Intrinsic Peroxidase Catalytic Activity and Its Application to Glucose Detection. *Adv. Mater.* **2010**, *22*, 2206−2210.
(47) He, W.; Wamer, W.; Xia, Q.; Yin, J.-j.; Fu, P. P. Enzyme-Like Activity of Nanomaterials. *J. Environ. Sci. Health, Part C: Environ. Carcinog. Ecotoxicol. Rev.* **2014**, *32*, 186−211.
(48) He, W.; Zhou, Y.-T.; Wamer, W. G.; Hu, X.; Wu, X.; Zheng, Z.; Boudreau, M. D.; Yin, J.-J. Intrinsic Catalytic Activity of Au Nanoparticles with Respect to Hydrogen Peroxide Decomposition and Superoxide Scavenging. *Biomaterials* **2013**, *34*, 765−773.
(49) He, W.; Zhou, Y.-T.; Wamer, W. G.; Boudreau, M. D.; Yin, J.-J. Mechanisms of the pH Dependent Generation of Hydroxyl Radicals and Oxygen Induced by Ag Nanoparticles. *Biomaterials* **2012**, *33*, 7547−7555.

DOI: 10.1021/acsami.5b05180
ACS Appl. Mater. Interfaces 2015, 7, 19709−19717

(50) Liu, Y.; Wu, H.; Li, M.; Yin, J.-J.; Nie, Z. pH Dependent Catalytic Activities of Platinum Nanoparticles with Respect to the Decomposition of Hydrogen Peroxide and Scavenging of Superoxide and Singlet Oxygen. *Nanoscale* **2014**, *6*, 11904−11910.
(51) Seo, S. Y.; Sharma, V. K.; Sharma, N. Mushroom Tyrosinase: Recent Prospects. *J. Agric. Food Chem.* **2003**, *51*, 2837−2853.
(52) Yoruk, R.; Marshall, M. R. Physicochemical Properties and Function of Plant Polyphenol Oxidase: A Review. *J. Food Biochem.* **2003**, *27*, 361−422.
(53) Priestley, G. C. *Molecular aspects of dermatology*; Molecular Medical Science Series; John Wiley and Sons Ltd.: Chichester, England, 1993; Book 3.
(54) Artes, F.; Castaner, M.; Gil, M. I. Review: Enzymatic Browning in Minimally Processed Fruit and Vegetables. *Food Sci. Technol. Int.* **1998**, *4*, 377−389.
(55) Vaclavik, L.; Krynitsky, A. J.; Rader, J. I. Targeted Analysis of Multiple Pharmaceuticals, Plant Toxins and Other Secondary Metabolites in Herbal Dietary Supplements by Ultra-High Performance Liquid Chromatography Quadrupole-Orbital Ion Trap Mass Spectrometry. *Anal. Chim. Acta* **2014**, *810*, 45−60.
(56) Formica, J. V.; Regelson, W. Review of the Biology of Quercetin and Related Bioflavonoids. *Food Chem. Toxicol.* **1995**, *33*, 1061−1080.
(57) Solomon, E. I.; Sundaram, U. M.; Machonkin, T. E. Multicopper Oxidases and Oxygenases. *Chem. Rev.* **1996**, *96*, 2563−2606.
(58) Kubo, I.; Nihei, K.; Shimizu, K. Oxidation Products of Quercetin Catalyzed by Mushroom Tyrosinase. *Bioorg. Med. Chem.* **2004**, *12*, 5343−5347.
(59) Zhou, Y.-T.; Yin, J.-J.; Lo, Y. M. Application of ESR Spin Label Oximetry in Food Science. *Magn. Reson. Chem.* **2011**, *49*, S105−S112.
(60) Korytowski, W.; Sarna, T.; Kalyanaraman, B.; Sealy, R. C. Tyrosinase-Catalyzed Oxidation of Dopa and Related Catechol(amine)s - a Kinetic Electron-Spin-Resonance Investigation Using Spin-Stabilization and Spin Label Oximetry. *Biochim. Biophys. Acta, Gen. Subj.* **1987**, *924*, 383−392.
(61) Rolff, M.; Schottenheim, J.; Decker, H.; Tuczek, F. Copper-O_2 Reactivity of Tyrosinase Models towards External Monophenolic Substrates: Molecular Mechanism and Comparison with the Enzyme. *Chem. Soc. Rev.* **2011**, *40*, 4077−4098.
(62) Olivares, C.; Solano, F. New Insights into the Active Site Structure and Catalytic Mechanism of Tyrosinase and Its Related Proteins. *Pigm. Cell Melanoma Res.* **2009**, *22*, 750−760.
(63) Ramsden, C. A.; Riley, P. A. Tyrosinase: The Four Oxidation States of the Active Site and Their Relevance to Enzymatic Activation, Oxidation and Inactivation. *Bioorg. Med. Chem.* **2014**, *22*, 2388−2395.
(64) Que, L., Jr.; Tolman, W. B. Biologically Inspired Oxidation Catalysis. *Nature* **2008**, *455*, 333−340.
(65) Gerdemann, C.; Eicken, C.; Krebs, B. The Crystal Structure of Catechol Oxidase: New Insight into the Function of Type-3 Copper Proteins. *Acc. Chem. Res.* **2002**, *35*, 183−191.
(66) Decker, H.; Schweikardt, T.; Tuczek, F. The First Crystal Structure of Tyrosinase: All Questions Answered? *Angew. Chem., Int. Ed.* **2006**, *45*, 4546−4550.
(67) Mallat, T.; Baiker, A. Oxidation of Alcohols with Molecular Oxygen on Solid Catalysts. *Chem. Rev.* **2004**, *104*, 3037−3058.
(68) Li, C.; Hoffman, M. Z. One-Electron Redox Potentials of Phenols in Aqueous Solution. *J. Phys. Chem. B* **1999**, *103*, 6653−6656.

DOI: 10.1021/acsami.5b05180
ACS Appl. Mater. Interfaces 2015, 7, 19709−19717